Zeolites

DOI: 10.1002/anie.201404608

An Extra-Large-Pore Zeolite with Intersecting 18-, 12-, and 10-Membered Ring Channels**

*Fei-Jian Chen, Yan Xu, and Hong-Bin Du**

Dedicated to Professor Xiao-Zeng You on the occasion of his 80th birthday

Abstract: *Zeolites with extra-large pores have attracted great attention because of their important applications such as in hydrocracking, catalysis, and separation of large molecules. Despite much progress has been made during the past decades, the synthesis of these materials remains a big challenge. A new extra-large-pore zeolite NUD-1 (Nanjing University Du's group zeolite no. 1) is synthesized by using an approach based on supramolecular self-assemblies of small aromatic organic cations as structure-directing agents. NUD-1 possesses interconnecting 18-, 12-, and 10-membered ring channels, built from the same building units as those of ITQ-33 and ITQ-44. There coexist single 3-membered ring, double-3-membered ring and double-4-membered ring secondary building units in NUD-1, which have not been seen in any other zeolites.*

Since the discovery of the iron aluminophosphate mineral cacoxenite with an open channel of 14.1 Å,[1] inorganic molecular sieves with extra-large pores (i.e. consisting of more than 12 tetrahedra) have attracted great attention because of their potential applications in, for example, hydroprocessing heavy oil fractions, facilitating the production of fine chemicals and biomass processes, shape-selective catalysis and separation of large molecules.[2] The first man-made molecular sieve containing an 18-membered ring (18-MR) is aluminophosphate VPI-5 (VFI, three letter structure code given by the International Zeolite Association), which was synthesized in 1988.[3] Since then, a number of new molecular sieves with extra-large pores have been synthesized, which include silicates, germinates, metal phosphates, and phosphites.[4] However, it remains a challenge to synthesize novel open inorganic frameworks with extra-large pores, particularly of the silicate zeolites. The silicate zeolites are the most promising materials for industrial applications because of their good stability and chemical properties. Up to date, there are only three known silicate/germanosilicate zeolites with pores larger than 18-MR channels amongst more than 200 structurally characterized zeolites, that is, ITQ-37 (30-MR),[5] ITQ-43 (28-MR),[6] and PKU-12 (-CLO, 20-MR).[7]

The past decade has witnessed the miraculous development and prosperity of the large and extra-large-pore zeolites,[4] owing to the use of germanium in the concentrated fluoride system during the synthesis. The F^- mineralizer has a tendency to stabilize the double-4-membered rings (D4Rs) in zeolites, while germanium favors the formation of the small cages like D3Rs and D4Rs because of the longer Ge–O bond length (ca. 1.74 Å) and smaller Ge-O-Ge angle (ca. 130°) compared with those of silicon (Si–O bond length ca. 1.61 Å and Si-O-Si angle ca. 145°).[8] These small rings/cages are thought to be the key to the formation of large and extra-large-pore zeolites according to the studies by Brunner and Maier.[9] They showed that zeolites with a low-density framework should contain a relatively large number of 3- and 4-MRs, and the low-density materials tend to have desirable large rings. So far, a large number of thermodynamically feasible, new low-density zeolites have been predicted by various computational studies,[10] which have stimulated the research on synthesizing large and extra-large-pore zeolites. Extra-large-pore zeolites ITQ-33[11] and ITQ-44,[12] for example, were first predicted by Foster and Treacy,[10b] and later successfully synthesized by Corma et al. The two structures possess the same stuffed cage-like structure building unit (SBU) [$3^2.4^3.6^9$] made of two 3-MRs, three 4-MRs and nine 6-MRs. The SBUs are linked together by bridging oxygen atoms between the 4-MRs and by either sharing the 3-MRs, or bridging oxygen atoms between the 3-MRs to form a three-dimensional framework. This gives rise to ITQ-33 with a pore system of $18\times10\times10$ MRs, or ITQ-44 with a pore system of $18\times12\times12$ MRs, respectively. Herein, we present the synthesis of a new zeolite NUD-1 (Nanjing University Du's group zeolite no. 1) with an extra-large pore of 18 MR, built on the same SBUs as those of ITQ-33 and ITQ-44. Interestingly, the SBUs in NUD-1 are instead connected together both by sharing the 3-MRs and by bridging oxygen atoms between the 3-MRs, thus leading to a new zeolite structure with a pore system of $18\times12\times10$-MRs.

NUD-1 was synthesized by using 1-methyl-3-(4-methylbenzyl)imidazolium (SDA1) as a structure-directing agent (SDA; see Table S1 in the Supporting Information) in the

[*] F.-J. Chen, Prof. H.-B. Du
State Key Laboratory of Coordination Chemistry, School of Chemistry and Chemical Engineering, Nanjing University
Nanjing, 210093 (China)
E-mail: hbdu@nju.edu.cn
Prof. Y. Xu
College of Chemistry and Chemical Engineering, State Key Laboratory of Materials-oriented Chemical Engineering, Nanjing Tech University
Nanjing, 210009 (China)

[**] We are grateful for financial support from the National Basic Research Program (grant number 2011CB808704) and the National Natural Science Foundation of China (grant number 21071075). The authors thank Drs. L.-T. Yang and A. Gerisch at Bruker AXS GmbH for collecting the single-crystal diffraction data, and X. K. Ke at Nanjing University for solid-state NMR measurements.

Supporting information for this article is available on the WWW under http://dx.doi.org/10.1002/anie.201404608.

presence of germanium and fluoride. The best crystallized, pure phase of NUD-1 was obtained with a gel composition of $1\,SiO_2$:$1\,GeO_2$:$0.8\,SDA1(OH)$:$0.8\,HF$:$10\,H_2O$ at 150 °C for 15 days. Large, hexagonal prism crystals of NUD-1 up to $45\times10\times10\ \mu m^3$ in sizes were obtained with 1-methyl-3-(naphthalen-2-ylmethyl)-imidazolium (SDA2) as an SDA (inset in Figure 1), from which suitable crystals were selected for single-crystal X-ray diffraction analysis. The X-ray powder diffraction (XRPD) pattern of NUD-1 calculated from the single-crystal structure data is in good agreement with those observed for the as-synthesized NUD-1 (Figure 1).

Single-crystal X-ray diffraction analysis reveals that NUD-1 crystallizes in a hexagonal space group *P6*/mmm,[13] the structure of which is built on the same stuffed cage-like SBU as that of ITQ-33 or ITQ-44. As shown in Figure 2a, the SBU is formed by three small [$4.5^2.6^2$] cages by sharing the T6-T7 edges, then capped by two 3-MRs from the top and the bottom, respectively. This gives rise to a triagonal bipyramid SBU [$3^2.4^3.6^9$], possessing two coordination-unsaturated 3-MRs (T3 and T8) locating at the apices and three coordination-unsaturated 4-MRs (T1 and T2) lying on the basal plane. The SBUs are aligned with the basal plane parallel to the *ab* plane and the principal axis of each triagonal bipyramid (passing through the T6-T7) coinciding with the 3-fold axis. The adjacent SBUs in the same basal plane are connected together by bridging oxygen atoms between the coordination-unsaturated 4-MRs, that is, by D4Rs, to form a 2-dimensional sheet with large 18-MR pores (Figure 2b). The identical sheets are also found in ITQ-33 and ITQ-44. It is, however, because of the different connection manners between the neighbouring sheets that results in different structures in the three zeolites. In ITQ-33 (Figure 2d), the adjacent layers are fused together by sharing the 3-MRs of the SBUs in each layer, which results in 10-MR pores along the *a* and *b* axes intersecting the 18-MR channels. On the other hand, the layers in ITQ-44 are connected by bridging oxygen atoms between the coordination-unsaturated 3-MRs (Figure 2e). This leads to the formation of D3Rs and 12-MR channels intersecting with the 18-MR pores. NUD-1, however, adopts

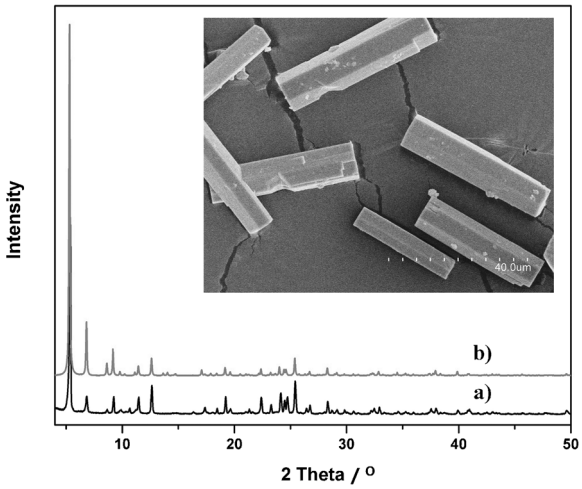

Figure 1. XRPD patterns of a) the as-synthesized and b) the calculated NUD-1 based on the single-crystal diffraction data. The inset shows a SEM image of SDA2-NUD-1 crystals (picture size about 100 μm).

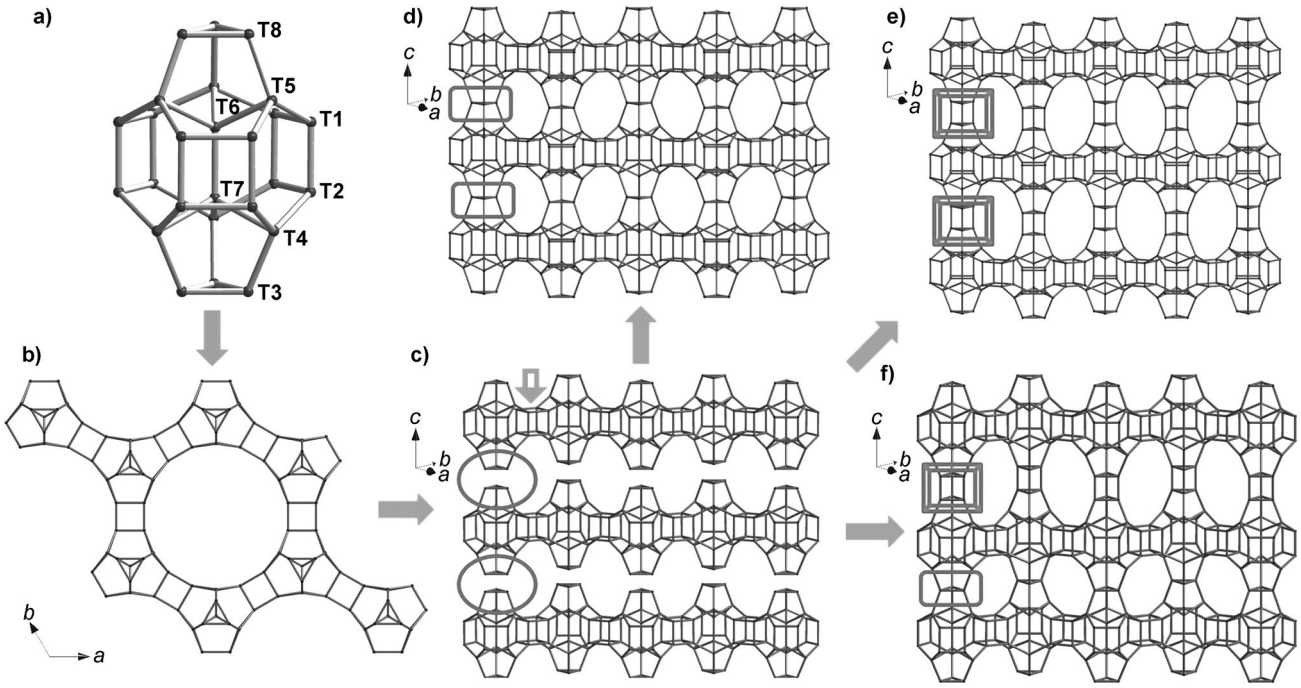

Figure 2. Structure of NUD-1. a) SBU of NUD-1, showing the locations of the eight independent T atoms. b) View of a single layer formed by the SBUs, showing the 18-MR channels along the [001] direction. c) Tilt view of three adjacent layers along the (110) direction, showing the D4R units (indicated by an arrow). d) ITQ-33: Condensation of the layers through the 3-MRs, forming the 10-MRs. e) ITQ-44: Connection of the layers by bridging O atoms on the 3-MRs, forming the D3Rs and the 12-MRs. f) NUD-1: Connection of the layers alternatively by 3-MRs and D3Rs, forming the 10-MRs and 12-MRs. The frames highlight the different connections in zeolites. Oxygen atoms have been omitted for clarity.

both ways of linking the neighboring layers: Each sheet is connected to the neighboring one by sharing the 3-MRs as in ITQ-33 on one side of the sheet, whereas on the other side it is connected to another neighboring sheet by bridging D3Rs as in ITQ-44. This results in a new three-dimensional zeolite possessing structure features of both ITQ-33 and ITQ-44 (Figure 2 f).

NUD-1 possesses a three-dimensional channel system with straight extra-large 18-MR channels along the *c* axis direction which are intersected by 10-MR and 12-MR channels running along the *a* and *b* axes (Figure S2). The crystallographic pore diameter of the 18-MR channel is 12.2 Å, similar to those found in ITQ-33 (12.2 Å) and ITQ-44 (12.5 Å), while the 10-MR and 12-MR channels have openings of 4.3×6.2 Å and 5.8×8.2 Å, respectively, very close to those of ITQ-33 (4.3×6.1 Å, 10-MR) and ITQ-44 (6.0×8.2 Å, 12-MR). The framework density of NUD-1 is 11.8 T atoms per 1000 $Å^3$, which is in between those of ITQ-33 (12.3 T) and ITQ-44 (10.9 T). From a topological point of view, the structure of NUD-1 can be considered as a known uninodal 5-connecting BN net (Figure S3), in which the SBU $[3^2.4^3.6^9]$ is considered as a 5-connecting triagonal bipyramid node.

NUD-1 contains single 3-MR, D3R and D4R units, which is unprecedented in any other known zeolites. At the center of each D4R, an F^- ion was located during structure refinement, while an hydroxyl ion was found at the center of each D3R, similar to the result of Monge and co-workers.[14] Consistently, the solid-state ^{19}F NMR spectra of the as-synthesized NUD-1 (Figure S4) showed a strong resonance band at −9.0 ppm owing to the F^- in D4Rs and a peak at −122.3 ppm for free F^- ion within the channels.[15] In the meanwhile, the solid-state ^{29}Si MAS NMR spectrum of the as-synthesized NUD-1 (Figure S5) showed a weak signal at −123.8 ppm originating from five-coordinate $SiO_{4/2}F^-$ units,[16] in addition to the peaks of tetrahedral framework silicons between −90 and −110 ppm. The structure refinements of the single-crystal diffraction data showed that there are preferential germanium occupancies at D3R and D4R units in NUD-1, similar to those of ITQ-33 and ITQ-44. As shown in Figure 2 a, there are eight crystallographically independent T-sites in NUD-1, rather than four as in ITQ-33 and ITQ-44. In respect of the coordination environments, the T5, T8, T6 and T1 positions in NUD-1 with Ge occupancies of 9, 0, 0, and 70%, respectively, resemble their respective counterparts in ITQ-33 (c.f. 33, 0, 0, and 39% of Ge). On the other hand, the T3, T4, T7, and T2 positions in NUD-1 consisting of 86, 33, 0, and 65% of Ge, respectively, are comparable to those of 50, 26, 0, and 37% of Ge observed in ITQ-44. Therefore, germanium in NUD-1 preferentially occupies the positions that are directly linked to D3Rs (T4) or on the D3Rs (T3) and D4Rs (T1 and T2), while it disfavors the positions that are directly linked to single 3-MRs (T5) or on the single 3-MRs (T8) and 5-MRs (T6 and T7). The chemical composition of the framework atoms obtained from the crystal structure refinement is $Ge_{47.81}Si_{50.19}O_{196}$, which matches well with the ICP result of $Ge/Si = 0.95$.

Due to the disorders, the organic cations were not located in the single-crystal structure model. However, the solid-state ^{13}C NMR spectra of the as-synthesized NUD-1 (Figure S6) showed that the organic SDA cations were included intact in the final product. Based on the crystal structure refinement, thermogravimetry (Figure S7), inductively coupled plasma (ICP), and CHN elemental analyses, the formula of the as-synthesized SDA2-NUD-1 can be calculated as $Ge_{47.81}Si_{50.19}O_{196}(C_{15}N_2H_{15}F)_{7.69}(C_{15}N_2H_{15}OH)_2$.

It is possible to incorporate Al into the framework of NUD-1 so that it can generate the acidic sites for potential catalytic applications. By using the synthesis procedure described above, the pure phase of Al-containing NUD-1 (Al-NUD-1) was obtained from the gel composition of $1\,SiO_2{:}1\,GeO_2{:}0.03\,Al_2O_3{:}1\,SDA1(OH){:}1\,HF{:}15\,H_2O$ at 150 °C for 15 d (Figure S8). The ^{27}Al MAS NMR spectrum of the as-synthesized Al-NUD-1 (Figure S9) showed the presence of a strong signal at 57 ppm with a negligible peak at 0 ppm. The results showed aluminium atoms present in the zeolite are tetrahedrally coordinated, suggesting that they are located in the framework positions.

The SDAs in NUD-1 can be removed by calcination in air at 550 °C while the structure remains intact (Figure S8). Like other germanosilicate zeolites, the calcined NUD-1 was not stable once left under the moisture condition, owning to the easy hydrolysis of the Ge−O bonds. In recent years, however, it has been shown that it is possible to decrease the Ge content or even obtain a pure silica polymorph during the synthesis with specially designed SDAs.[17] Moreover, the post-synthesis treatment such as isomorphous substitution of Al or Si for Ge has been proven to be an efficient, useful method to yield highly stable aluminosilicate or siliceous zeolites.[18] Work on NUD-1 in this aspect is in progress.

The N_2 adsorption of the calcined NUD-1 (Figure S10) gave the Brunauer–Emmett–Teller (BET) surface area of 646 m^2g^{-1}, and the *t*-Plot micropore volume of 0.26 cm^3g^{-1}. Partly because of a higher Ge content in NUD-1, the BET surface area is slightly lower than that of ITQ-33 (690 m^2g^{-1}) but higher than that of ITQ-44 (470 m^2g^{-1}). The estimated textural properties for the pure silica polymorph of NUD-1 would be 880 m^2g^{-1} for the BET surface area and 0.35 cm^3g^{-1} for micropore volume because of the lower atomic weight of silicon compared to germanium. The pore-size distribution obtained by applying the Howarth–Kamazoe formalism[19] to the Ar adsorption isotherm showed that NUD-1 possesses three different kinds of pore channels with pore sizes of 5.5, 6.8, and 10.4 Å, respectively, in accordance with the single-crystal structure model (Figure S11).

Finally, we noted that the formation of NUD-1 may involve supramolecular self-assemblies of SDAs, similar to those observed by Corma et al.[17a] and Gómez-Hortigüela et al.[20] during the syntheses of LTA-type germanosilicate ITQ-29 and aluminophosphate $AlPO_4$-5, respectively. This was confirmed by photoluminescent spectroscopy studies of the SDAs in diluted and concentrated solution, and the as-synthesized zeolites (Figure S12 and S13). The main emission bands of the SDA monomers in the hydroxide form in diluted solution appeared at ca. 330 nm. The SDA in the concentrated solution with the same concentration as for the synthesis of NUD-1 zeolite emitted at ca. 430 nm, attributable to the formation of excimers. The same emission bands were observed in the as-synthesized NUD-1 zeolite. These suggest

that the self-assembled aggregates of aromatic-containing cations were formed during the zeolite synthesis and acted as actual SDAs for the formation of NUD-1. It is worthy of note that, although the concept of self-assembled supramolecular aggregates as SDAs has been demonstrated previously, this work presents the first example of a new, extra-large-pore zeolite synthesized by this approach.

In conclusion, using easily prepared, small, and simple aromatic-containing imidazolium SDAs we have successfully synthesized a new extra-large-pore zeolite NUD-1 with interconnecting 18-, 12-, and 10-MR channels. The structure of NUD-1 is closely related to those of ITQ-33 and ITQ-44; the three zeolites are built from different stacking of the same building layer. NUD-1 consists of single 3-MR, D3R, and D4R units, which has not been observed in any other known zeolites. This study demonstrated that the use of supramolecular aggregates of aromatic-containing cations as SDAs can be employed to synthesize new extra-large-pore zeolites.

Experimental Section

The syntheses of SDAs are given in the Supporting Information. Zeolite NUD-1 was synthesized from the gel with a molar composition of $1\,SiO_2$:$x\,GeO_2$:y SDA(OH):y HF:$z\,H_2O$, where $x = 1$–0.2, $y = 1$–0.5, and $z = 3$–10 at 150 °C for 15 days. Further details are given in the Supporting Information.

X-ray powder diffraction (PXRD) data were collected on a Bruker D8 Advance instrument using a $Cu_{K\alpha}$ radiation ($\lambda = 1.54056$ Å) at room temperature. Elemental analyses of C, H, and N were performed on an Elementar Vario MICRO Elemental Analyzer. The inductively coupled plasma (ICP) analysis was carried out on a PerkinElmer Optima 3300 DV. Thermogravimetric analyses (TGA) were performed on a PerkinElmer thermal analyzer under air with a heating rate of 5 °C min^{-1}. A Micromeritics ASAP 2020 surface area porosimetry system was used to measure N_2 gas adsorption at 77 K. Scanning electron microscopy (SEM) images of the products were obtained on a field emission scanning electron microanalyzer (Hitachi S-4800), employing an accelerating voltage of 10 kV. Fluorescence measurements were performed on FluoroMax-4 spectrofluorometer with 3 nm slit for both excitation and emission. Liquid ^{13}C NMR spectra were recorded on Bruker DRX-500. Solid-state NMR spectra were recorded on a Bruker Av-400 spectrometer using magic-angle spinning (MAS) techniques at room temperature. ^{19}F NMR spectra were measured at 376.47 MHz in 4.0 mm diameter zirconia rotors at a spinning rate of 14 kHz. The spectra were collected using 2.1 μs pulses, which correspond to a magnetization flip angle of π/2 rad and a recycle delay of 15 s; the spectra were referenced to $CFCl_3$. The ^{13}C spectra were acquired at 100.62 MHz resonance frequency using a cross-polarization (CP) MAS sequence, with a 3.0 μs ^1H excitation pulse, 2.0 ms contact time, 5 s recycle delay, and 100 kHz spectral width, using proton decoupling at 60 kHz spinal64 during acquisition. The ^{29}Si MAS NMR spectra were acquired at a resonance frequency of 79.49 MHz with a π/8 pulse at 56 kHz, spectral width of 100 kHz, and 20 s relaxation delay. Solid-state ^{27}Al MAS NMR spectra were recorded on a Varian Unity VXR-400WB spectrometer at 104.2 MHz, with a π/18 rad pulse length, a recycle delay of 0.5 s, and spinning rate of 14 kHz.

The data collections for single-crystal X-ray diffraction for NUD-1 were carried out on a Bruker D8 VENTURE with TURBO X-RAY SOURCE $Cu_{K\alpha}$ radiation ($\lambda = 1.54178$ Å) at 100 K, with an exposure time of 60 s in a shutterless mode. The detector distance is 50 mm, while the scan width is 0.5°. Data reductions and absorption corrections were performed using the SAINT and SADABS programs,[21] respectively. Additional superstructure reflections that would double the *c*-axis were not taken into further account because of the low intensity. The structures were solved by direct methods using the SHELXS-97 program and refined with full-matrix least squares on F^2 using the SHELXL-97 program.[22] The organic cations and/or solvent molecules were not taken into account and squeezed out by PLATON/SQUEEZE.[23] All non-hydrogen atoms were refined anisotropically. Slightly large isotropic factors for the T8 and O15 positions at the single 3-MRs were found, which may be due to the presence of the superstructure. The largest peak in the final difference electron density synthesis was 3.63 e$^-$ Å^{-3} and the largest hole was −2.847 e$^-$ Å^{-3} with an RMS deviation of 0.168 e$^-$ Å^{-3}, which were located near the T8 and O15 positions. Details of the crystal parameters, data collection and refinement results are summarized in Table S2. The atomic coordinate data and selected bond lengths and angles are shown in Tables S3 and S4, respectively.

Received: April 23, 2014
Revised: June 3, 2014
Published online: July 11, 2014

Keywords: silicates · structure elucidation · synthesis design · templates · zeolites

[1] P. B. Moore, J. Shen, *Nature* **1983**, *306*, 356–358.
[2] a) X. Gao, Z. Qin, B. Wang, X. Zhao, J. Li, H. Zhao, H. Liu, B. Shen, *Appl. Catal. A* **2012**, *413–414*, 254–260; b) A. Corma, S. Iborra, A. Velty, *Chem. Rev.* **2007**, *107*, 2411–2502.
[3] M. E. Davis, C. Saldarriaga, C. Montes, J. Garces, C. Crowder, *Nature* **1988**, *331*, 698–699.
[4] J. Jiang, J. Yu, A. Corma, *Angew. Chem.* **2010**, *122*, 3186–3212; *Angew. Chem. Int. Ed.* **2010**, *49*, 3120–3145.
[5] J. Sun, C. Bonneau, A. Cantin, A. Corma, M. J. Diaz-Cabanas, M. Moliner, D. Zhang, M. Li, X. Zou, *Nature* **2009**, *458*, 1154–1157.
[6] J. Jiang, J. L. Jorda, J. Yu, L. A. Baumes, E. Mugnaioli, M. J. Diaz-Cabanas, U. Kolb, A. Corma, *Science* **2011**, *333*, 1131–1134.
[7] J. Su, Y. Wang, J. Lin, J. Liang, J. Sun, X. Zou, *Dalton Trans.* **2013**, *42*, 1360–1363.
[8] M. O'Keeffe, O. M. Yaghi, *Chem. Eur. J.* **1999**, *5*, 2796–2801.
[9] G. O. Brunner, W. M. Meier, *Nature* **1989**, *337*, 146–147.
[10] a) M. W. Deem, R. Pophale, P. A. Cheeseman, D. J. Earl, *J. Phys. Chem. C* **2009**, *113*, 21353–21360; b) M. D. Foster, M. M. J. Treacy, http://www.hypotheticalzeolites.net/.
[11] A. Corma, M. J. Diaz-Cabanas, J. L. Jorda, C. Martinez, M. Moliner, *Nature* **2006**, *443*, 842–845.
[12] J. Jiang, J. L. Jorda, M. J. Diaz-Cabanas, J. Yu, A. Corma, *Angew. Chem.* **2010**, *122*, 5106–5108; *Angew. Chem. Int. Ed.* **2010**, *49*, 4986–4988.
[13] Crystal data for NUD-1: $H_{10}F_6Ge_{47.81}O_{198}Si_{50.19}$, $M = 8172.44$, hexagonal, $a = 19.2571(9)$ Å, $b = 19.2571(9)$ Å, $c = 25.9826(14)$ Å, $\gamma = 120°$, $V = 8344.4(10)$ Å^3, $T = 100(2)$ K, space group P6/mmm, $Z = 1$, 47091 reflections measured, 3324 independent reflections ($R_{int} = 0.0880$). The final R_1 and $wR(F^2)$ values were 0.0665 and 0.1637 for $I > 2\sigma(I)$, and 0.0834 and 0.1735 for all data, respectively. The goodness of the fit on F^2 was 1.109. Further details on the crystal structure investigations may be obtained free of charge from The Cambridge Crystallographic Data Centre via www.ccdc.cam.ac.uk/data_request/cif, by quoting the depository number CCDC 998761 which contains the supplementary crystallographic data for this paper.
[14] C. Cascales, E. Gutierrez-Puebla, M. Iglesias, M. A. Monge, C. Ruiz-Valero, N. Snejko, *Chem. Commun.* **2000**, 2145–2146.
[15] G. Sastre, J. A. Vidal-Moya, T. Blasco, J. Rius, J. L. Jordá, M. T. Navarro, F. Rey, A. Corma, *Angew. Chem.* **2002**, *114*, 4916–4920; *Angew. Chem. Int. Ed.* **2002**, *41*, 4722–4726.

[16] H. Koller, A. Wölker, L. A. Villaescusa, M. J. Díaz-Cabañas, S. Valencia, M. A. Camblor, *J. Am. Chem. Soc.* **1999**, *121*, 3368 – 3376.
[17] a) A. Corma, F. Rey, J. Rius, M. J. Sabater, S. Valencia, *Nature* **2004**, *431*, 287 – 290; b) A. Cantín, A. Corma, M. J. Diaz-Cabanas, J. L. Jordá, M. Moliner, *J. Am. Chem. Soc.* **2006**, *128*, 4216 – 4217; c) Á. Cantín, A. Corma, M. J. Díaz-Cabañas, J. L. Jordá, M. Moliner, F. Rey, *Angew. Chem.* **2006**, *118*, 8181 – 8183; *Angew. Chem. Int. Ed.* **2006**, *45*, 8013 – 8015.
[18] a) F. Gao, M. Jaber, K. Bozhilov, A. Vicente, C. Fernandez, V. Valtchev, *J. Am. Chem. Soc.* **2009**, *131*, 16580 – 16586; b) H. Xu, J.-G. Jiang, B. Yang, L. Zhang, M. He, P. Wu, *Angew. Chem.* **2014**, *126*, 1379 – 1383; *Angew. Chem. Int. Ed.* **2014**, *53*, 1355 – 1359; c) L. Burel, N. Kasian, A. Tuel, *Angew. Chem.* **2014**, *126*, 1384 – 1387; *Angew. Chem. Int. Ed.* **2014**, *53*, 1360 – 1363.
[19] G. Horváth, K. Kawazoe, *J. Chem. Eng. Jpn.* **1983**, *16*, 470 – 475.
[20] a) T. Álvaro-Muñoz, F. López-Arbeloa, J. Pérez-Pariente, L. Gómez-Hortigüela, *J. Phys. Chem. C* **2014**, *118*, 3069 – 3077; b) L. Gómez-Hortigüela, F. López-Arbeloa, F. Corà, J. Pérez-Pariente, *J. Am. Chem. Soc.* **2008**, *130*, 13274 – 13284; c) L. Gómez-Hortigüela, S. Hamad, F. López-Arbeloa, A. B. Pinar, J. Pérez-Pariente, F. Corà, *J. Am. Chem. Soc.* **2009**, *131*, 16509 – 16524.
[21] SMART and SADABS, Bruker AXS Inc., Madison, Wisconsin, USA, **1997**.
[22] G. M. Sheldrick, *Acta Crystallogr. Sect. A* **2008**, *64*, 112 – 122.
[23] A. L. Spek, *J. Appl. Crystallogr.* **2003**, *36*, 7 – 13.

